

Supplementary Information

An aperiodic chiral tiling by topological molecular self-assembly

Jan Voigt, Miloš Baljžović, Kévin Martin, Christian Wäckerlin, Narcis Avarvari* &
Karl-Heinz Ernst*

*Corresponding authors. Email: karl-heinz.ernst@empa.ch, narcis.avarvari@univ-angers.fr

Contents:

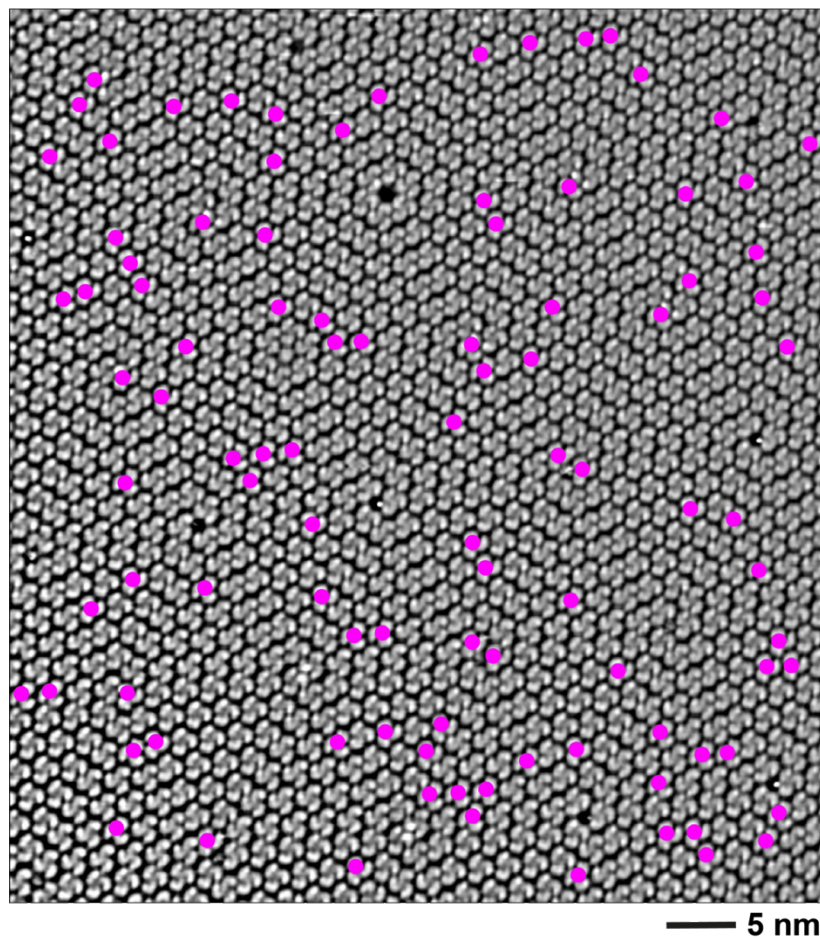
Supplementary Figs. 1-16

Supplementary Tables 1-2

Supplementary Equation 1

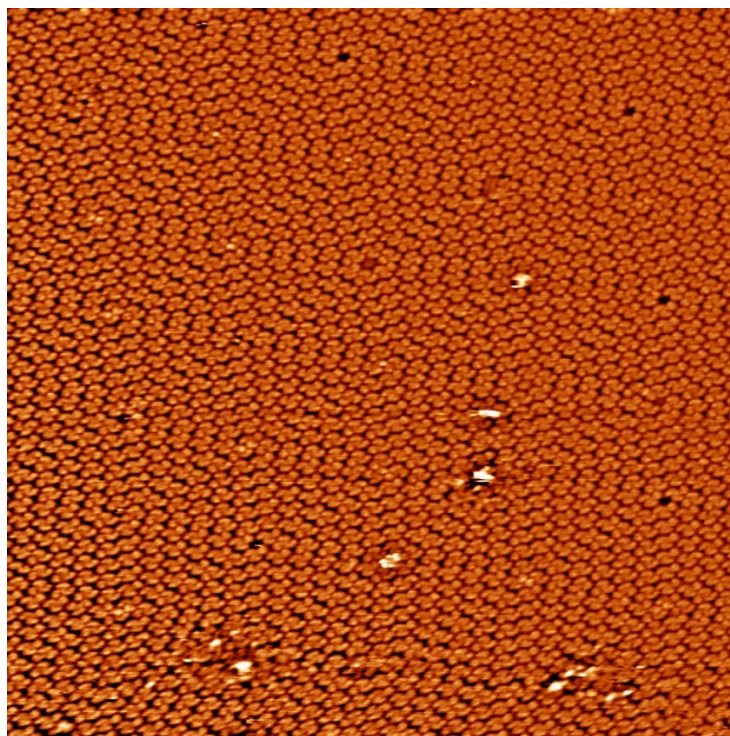
Supplementary Figures

Supplementary Fig. 1



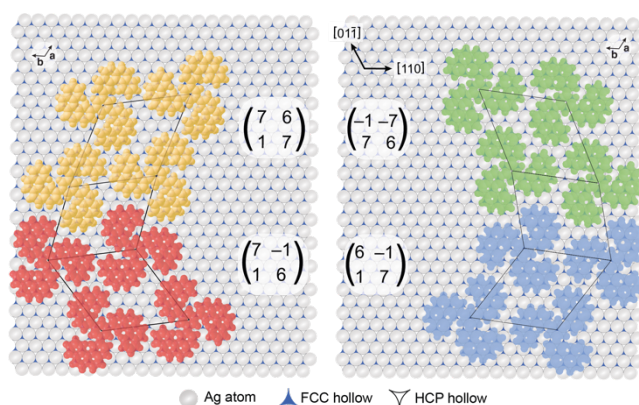
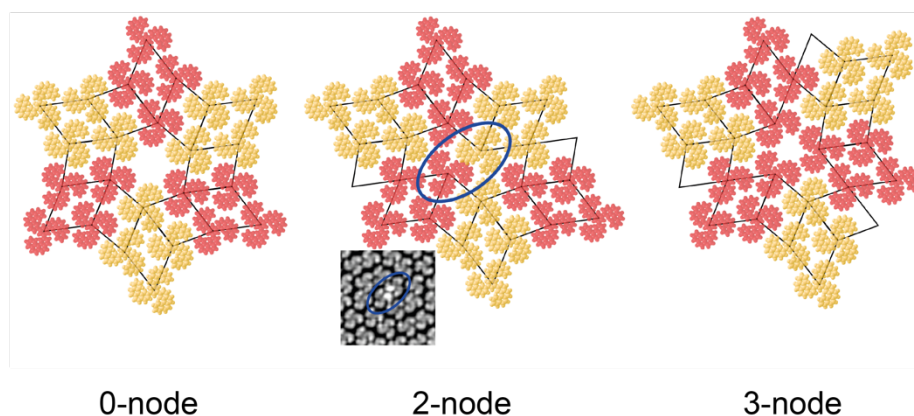
Supplementary Fig. 1 | Solid solution of enantiomers. (*P*)-enantiomers are marked with filled cyan circles for this domain with (*M*)-enantiomers as majority. The shown area is identical to the area shown in Fig. 1b.

Supplementary Fig. 2



Supplementary Fig. 2 | Mirror domain assembly. STM image (50 nm \times 50 nm, no drift correction) of an area showing the opposite 'mirror world' assembly with respect to Fig.1b. The image has been taken from the same preparation but hundreds of μm away from the area shown in Fig. 1b.

Supplementary Fig. 3

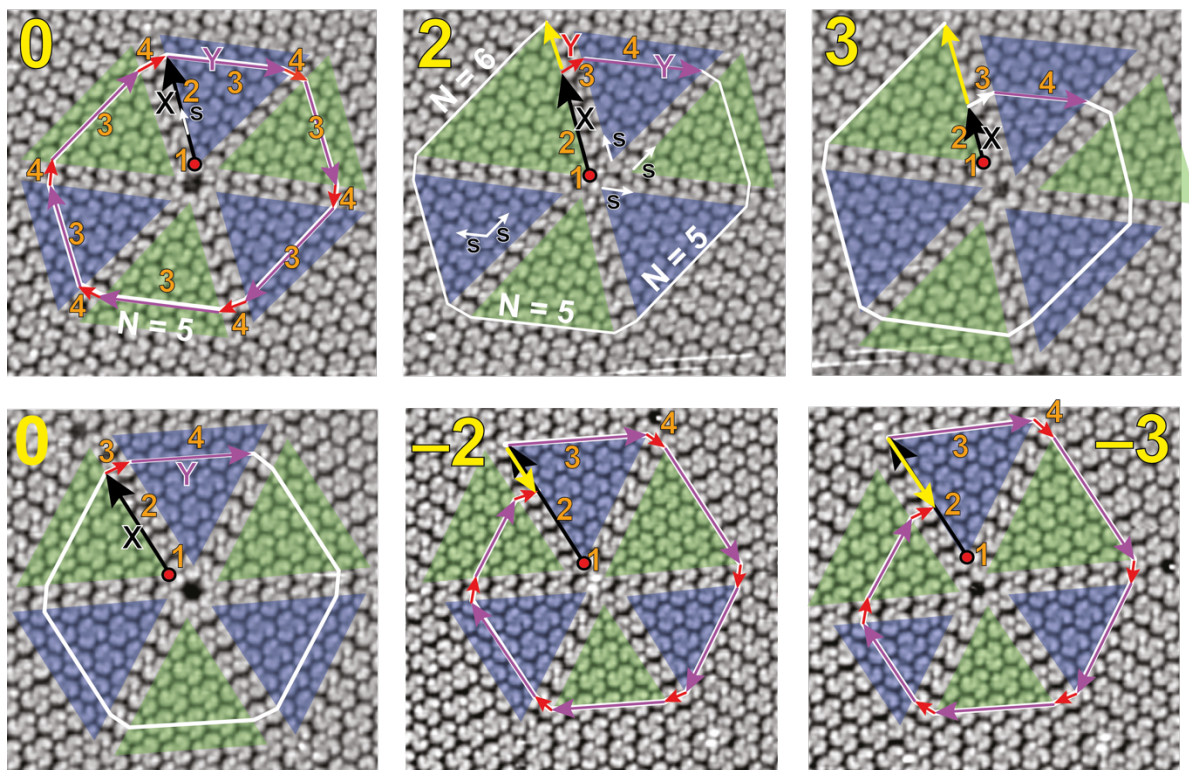


Supplementary Fig. 2 | Structure models of arrangements at nodes and triangle boundaries.

Top row: The molecular arrangements around the nodes show either voids (0- and 3-node) or overcrowding (2-node). The STM image for the 2-node suggests that two tetrahelicene arms of two molecules are bent upward.

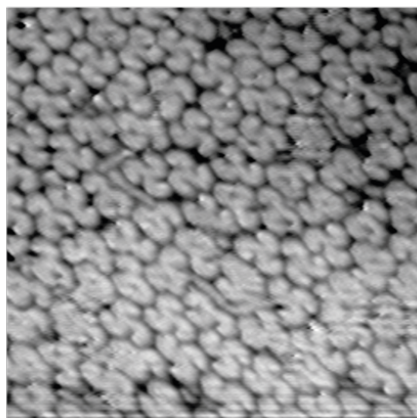
Bottom row: Closer interdigitation at the boundaries of triangles is achieved by relative rotation of the molecules by 60° . Within the triangles the molecules are arranged hexagonally. The matrix notation, relating the Ag(111) substrate lattice with the molecular lattice periodicity, is given for all four possible arrangements. Due to the 60° rotation molecules of adjacent triangles are placed on different adsorption sites and the entire arrangement becomes incommensurate with the Ag lattice. The intermolecular distance between equally colored molecules amounts to 1.85 nm.

Supplementary Fig. 4



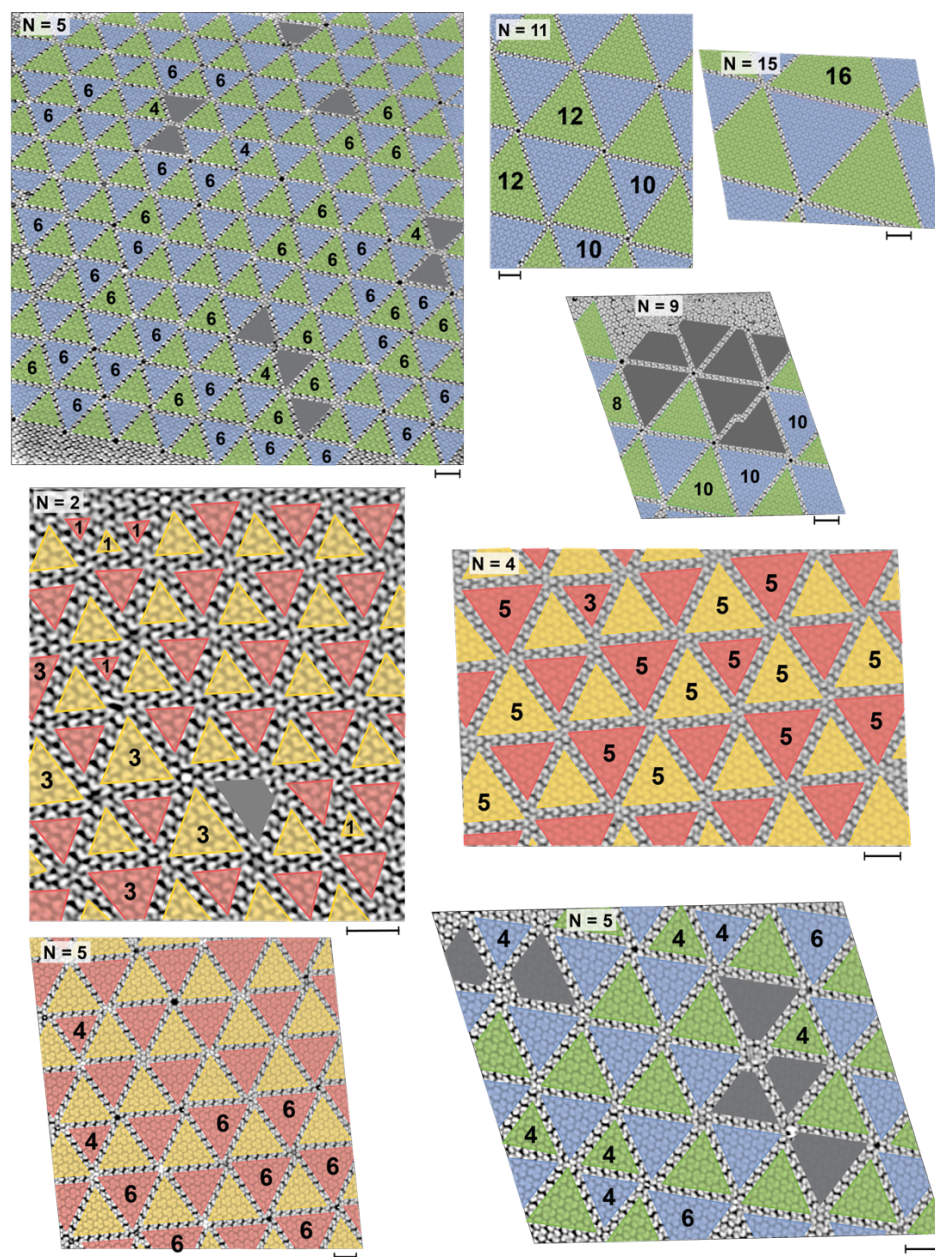
Supplementary Fig. 2 | Topology of nodes. In order to determine the topology of the three different observed nodes the following procedure is applied: As each node is the result of the arrangement of six triangles with hexagonally ordered molecules, the inner tip of one of the triangles serves as starting point (red dot, 1). From there draw a vector (**X**) along the edge of the triangle of several molecular unit vectors **s** (2). The length of **X** has to be between the triangle size $N-1$ and $N-3$ ($s \times N-1 \geq X \geq s \times N-3$; N = triangle size in units of **s**). All following operations are performed clockwise. From there draw a vector **Y** across the triangle to the opposite border with same distance to the inner triangle tip (3). Move to adjacent triangle border molecule that is closest (interdigitated) to last molecule (4). Repeat steps 3 and 4 until crossing a vector pointing at the same direction as **X**. If **X** was chosen on the right side of a triangle, order of steps 3 and 4 need to be invers (i.e. crossing to adjacent triangle border before moving across triangle). The topology is now defined by the distance in molecular unit vectors **s** of the endpoint of the operation to the tip of **X** (no matter if the endpoint is closer or farther away from the inner triangle tip). Nodes in a domain with the (*P*)-enantiomer as majority can have topologies of 0, 2 and 3; for nodes in domains with the (*M*)-enantiomer as majority topologies of 0, -2 and -3 are the result.

Supplementary Fig. 5



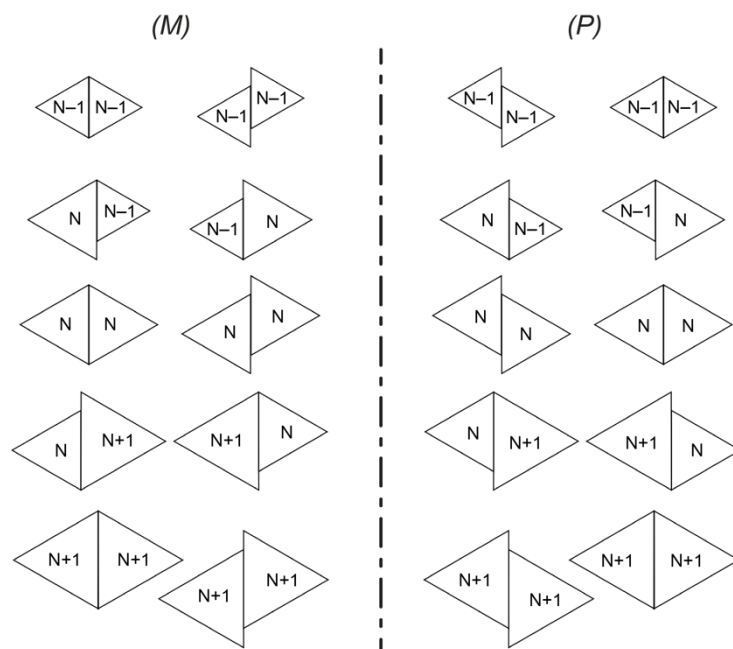
Supplementary Fig. 5 | Cold sample deposition. STM image (15 nm × 15 nm) after deposition at 170 K and cooling to 130 K. Even at high coverage there is no order. Not all molecules are present in their (M,M,M) - and (P,P,P) -configurations but also as diastereomers with mixed handedness, e.g. as (M,P,P) - or as (P,M,M) -isomers, appearing therefore in y-shapes.

Supplementary Fig. 6



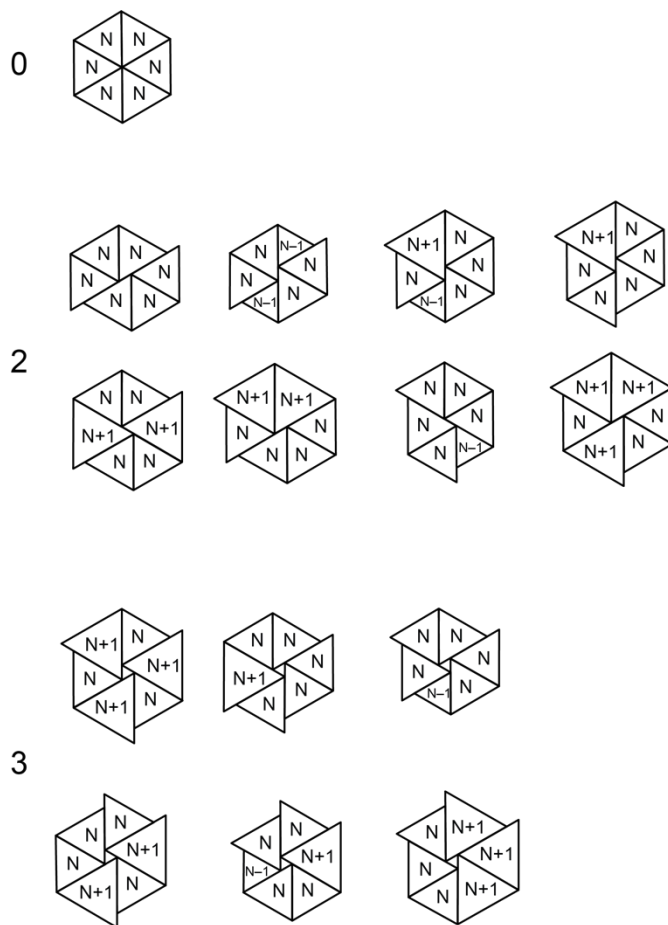
Supplementary Fig. 6 | $N \pm 1$ triangular phases. Examples of STM images acquired from different $N \pm 1$ triangular phases obtained after different identical sample preparations. Semitransparent triangles indicate corresponding color for molecular azimuthal orientation and majority. All STM images were drift corrected, causing the deviation from rectangular shape. The dominating N is indicated, while examples of the subordinate-sized ± 1 triangles are directly labeled. Incomplete triangles are labeled in grey. Scale bars below the images mark 5 nm.

Supplementary Fig. 7



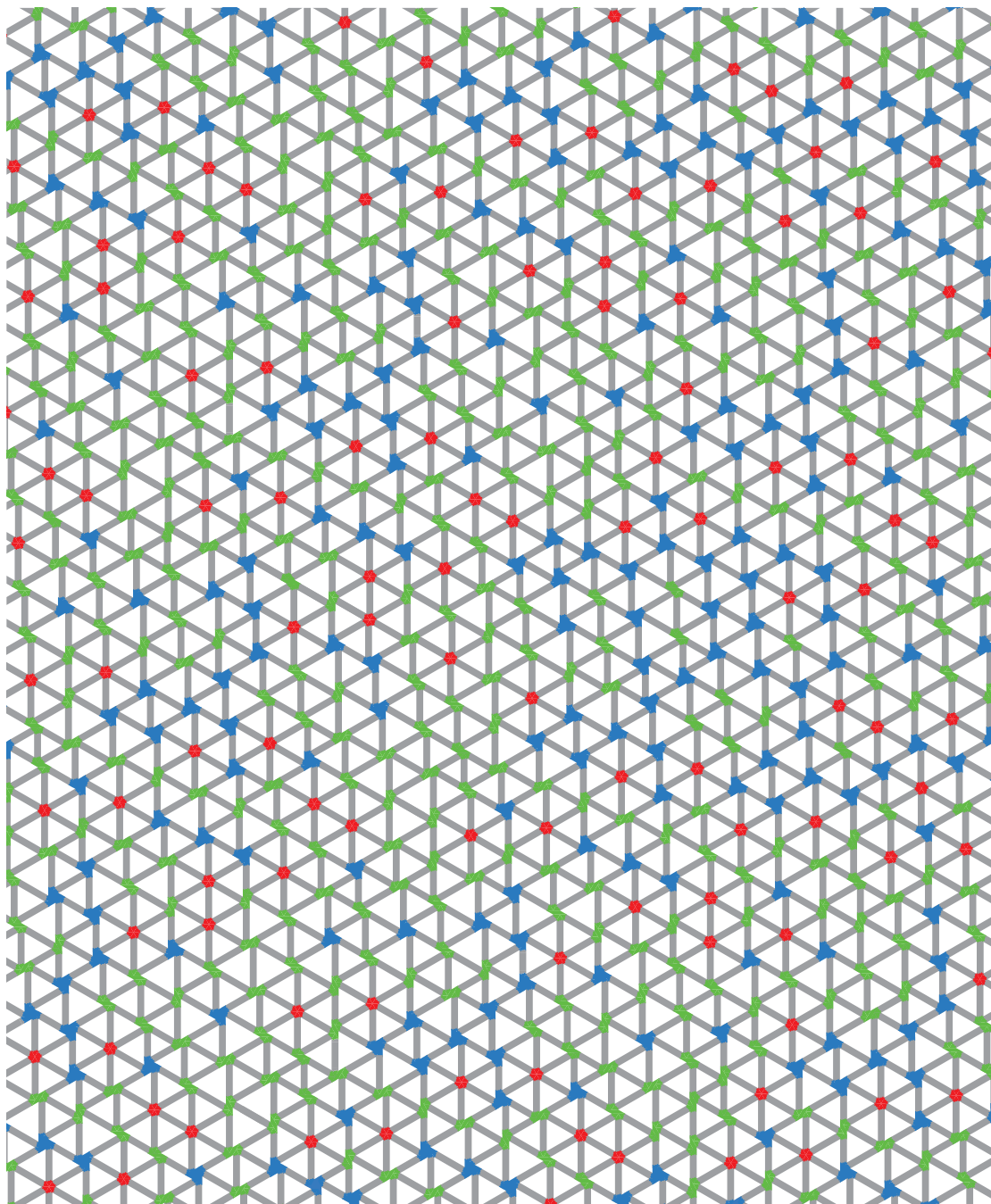
Supplementary Fig. 7 | Combinations of triangle arrangements in $N \pm 1$ topological assembly. 10 possible combinations are identified for each enantiomer. The enantiomer defines the direction of the offset between triangles.

Supplementary Fig. 8



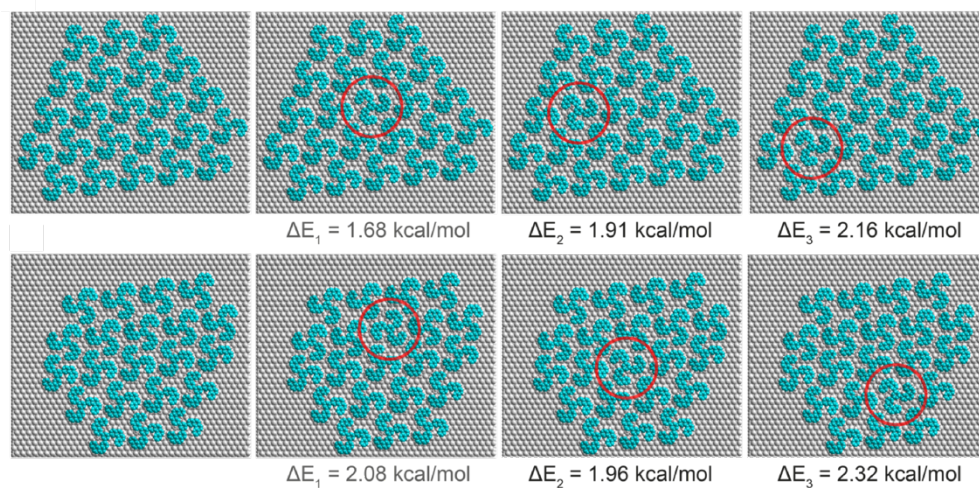
Supplementary Fig. 8 | Observed node types for triangular $N \pm 1$ topological assembly. More node types are theoretically possible but have not been identified experimentally.

Supplementary Fig. 9



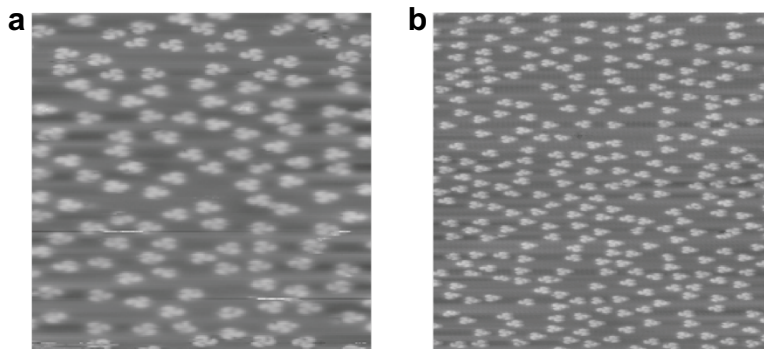
Supplementary Fig. 9 | Topological jigsaw tiling game. Example of an aperiodic tiling using the tile set introduced in Fig. 2f based on the $N \pm 1$ triangle size topology (triangle colors are kept in white).

Supplementary Fig. 10



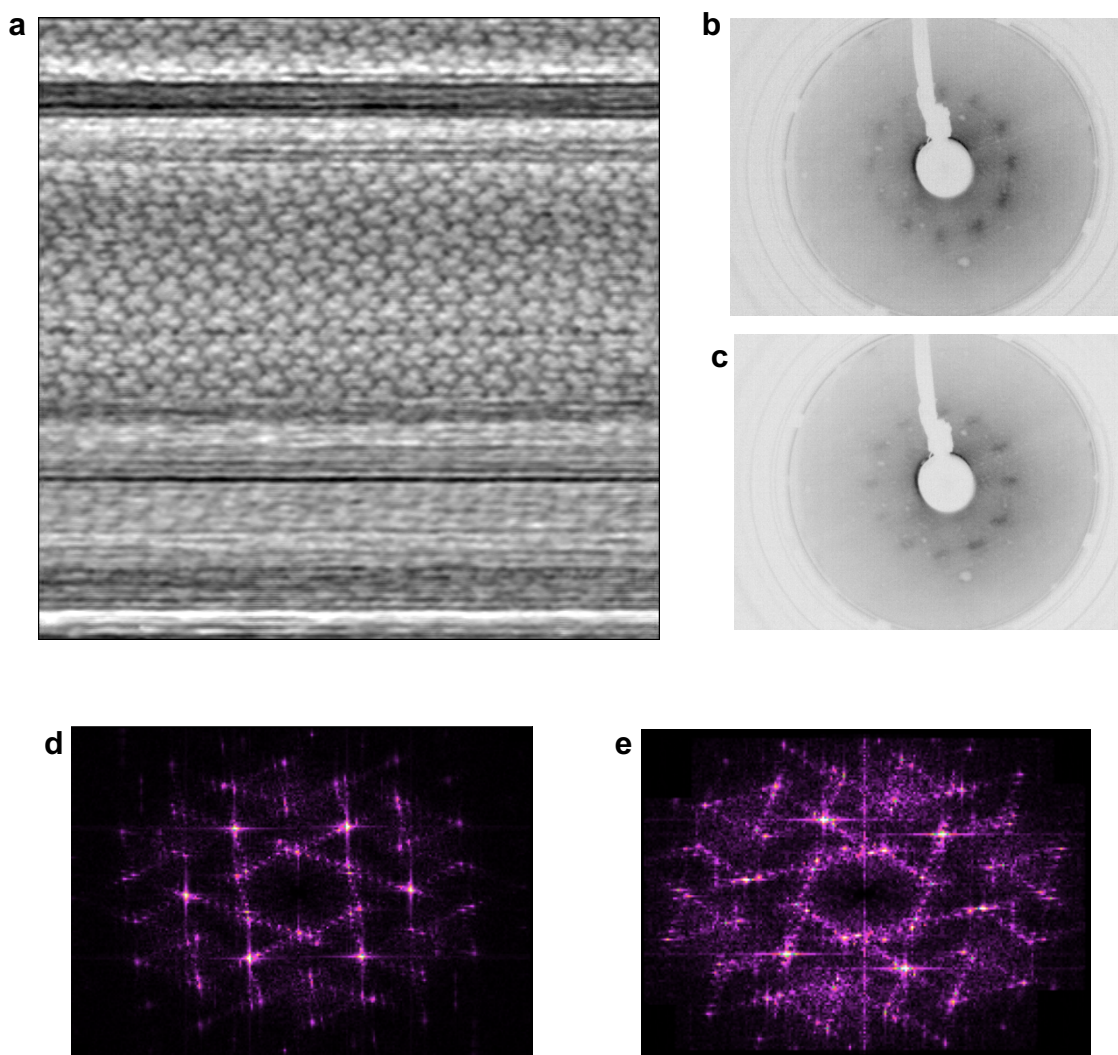
Supplementary Fig. 10 | Molecular mechanics of inclusion of a wrong enantiomer. The inclusion of a molecule with opposite handedness induces an energy penalty of only around 2 kcal/mol. The position within a given ensemble leads only to a small variation of this value.

Supplementary Fig. 11



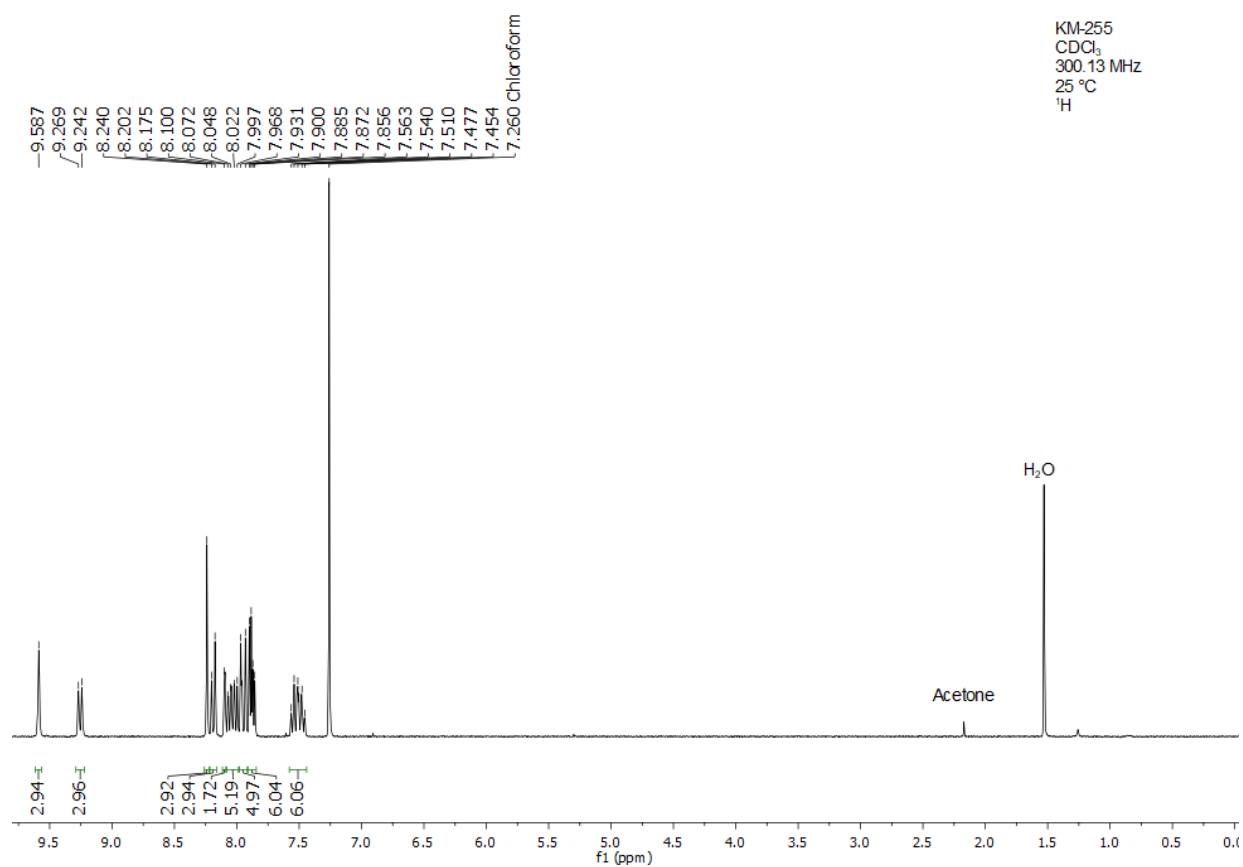
Supplementary Fig. 11 | Low-temperature STM investigation. **a**, STM image (50 nm \times 50 nm, $T = 10$ K) at low coverage after deposition at room temperature. Cooling rate: ~ 0.22 K/s. **b**, STM image (80 nm \times 80 nm, $T = 10$ K) at low coverage after deposition at room temperature. Cooling rate: ~ 0.22 K/s. The absence of aggregation into islands suggests very small attractive interactions and molecules interact basically only close to full monolayer coverage.

Supplementary Fig. 12



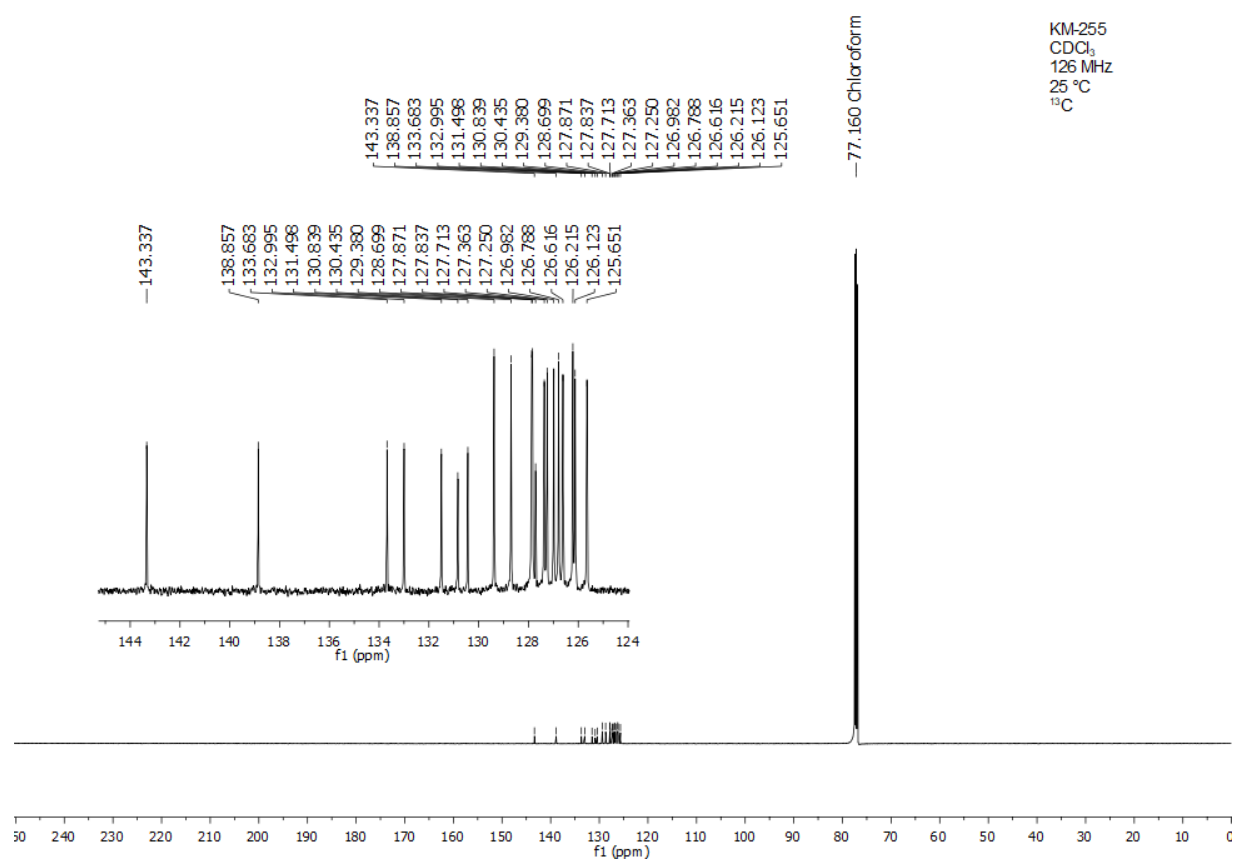
Supplementary Fig. 12 | Order at high temperature. **a**, STM image ($30\text{ nm} \times 30\text{ nm}$) of a closed-packed layer at room temperature. **b**, Low-energy electron diffraction (LEED, $E = 43\text{ eV}$) pattern of a monolayer at $40\text{ }^{\circ}\text{C}$. **c**, LEED pattern ($E = 43\text{ eV}$) of a monolayer at $80\text{ }^{\circ}\text{C}$. **d**, Inverse Fourier transformation of STM image of triangular phase containing excess of $(P)\text{-t[4]HB}$. **e**, Inverse Fourier transformation of STM image of triangular phase containing excess of $(M)\text{-t[4]HB}$.

Supplementary Fig. 13



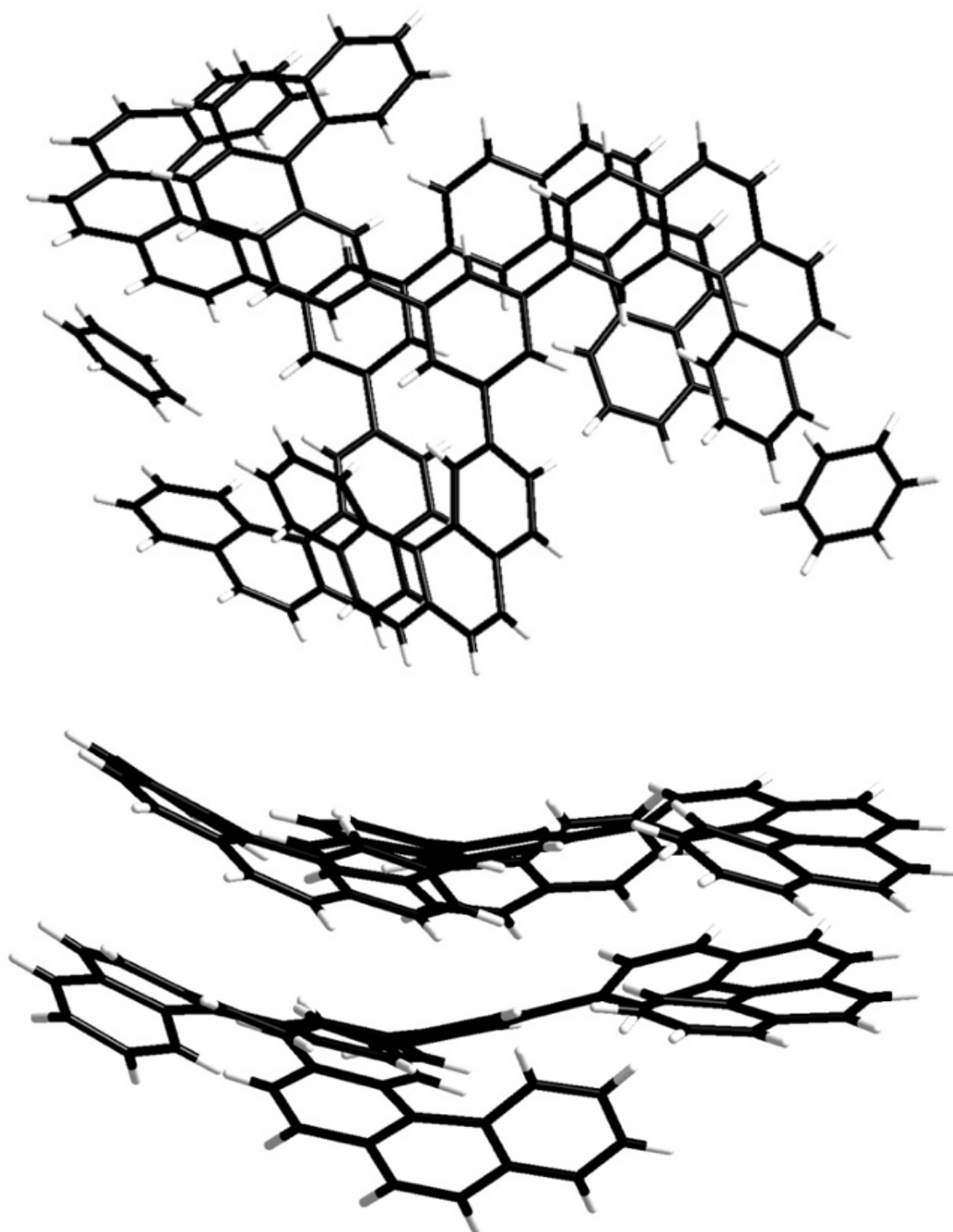
Supplementary Fig. 13 | ¹H NMR of t[4]HB.

Supplementary Fig. 14



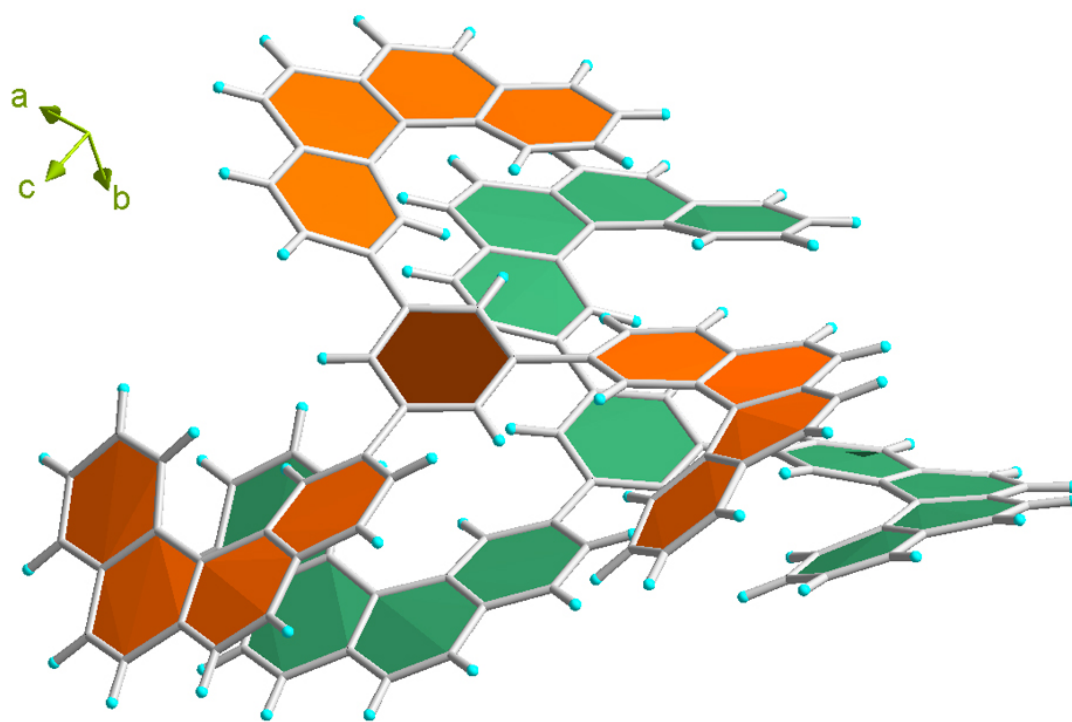
Supplementary Fig. 14 | 13C NMR of t[4]HB

Supplementary Fig. 15



Supplementary Fig. 15 | View of the molecular structure of t[4]HB (top); lateral view where the crystallization benzene molecules have been omitted (bottom).

Supplementary Fig. 16



Supplementary Fig. 16 | View of the two independent tris(helicene) molecules in the structure of t[4]HB.

Supplementary Table 1

Figure	U [V]	I [pA]
Fig1B	0.30	200
Fig1C -top	0.30	200
Fig1C - bottom	0.30	190
Fig1D	0.30	200
Fig1E	0.83	130
Fig 1E insets	0.30	200
Fig2D -top	0.30	200
Fig2D - bottom	0.30	190
Fig3A	0.78	560
Fig3C	0.30	200
Fig3D-left	0.96	360
Fig3D-right	0.85	210
FigS1	0.30	200
FigS2	0.30	200
FigS4 (N=5, top)	0.25	260
FigS4 (N=11)	0.83	130
FigS4 (N=15)	0.42	540
FigS4 (N=9)	0.42	620
FigS4 (N=2)	0.50	150
FigS4 (N=4)	0.39	120
FigS4 (N=5, left)	0.30	200
FigS4 (N=5, right)	0.30	190
FigS8A	0.48	500
FigS8B	1.12	360
FigS8C	0.594	250
Fig.S9A	1.25	60

Supplementary Table 1 | STM parameters of all presented STM images.

Supplementary Table 2

Formula	C ₁₂₉ H ₈₁
Molecular Weight	1630.93
Temperature (K)	150.0(1)
Wavelength (Å)	1.54184
Crystal system	Monoclinic
Space group	<i>P</i> 2 ₁ / <i>c</i>
a (Å)	25.014(2)
b (Å)	7.5767(5)
c (Å)	44.880(4)
α (°)	90
β (°)	103.338(9)
γ (°)	90
V (Å ³)	8276.4(12)
Z	4
Crystal color	Colourless
Crystal size (mm ³)	0.3 x 0.2 x 0.1 mm
D _c (g cm ⁻³)	1.309
F(000)	3420
μ (mm ⁻¹)	0.563
Transmission (min/max)	0.65353/1.00000
θ (min/max) (°)	2.386/76.2
Data collected	34412
Data unique	16780
Data observed	8676
R (int)	0.0829
Nb of parameters	1162
Nb of restraints	0
R ₁ [I > 2σ(I)]	0.0827
wR ₂ [I > 2σ(I)]	0.1963
R ₁ [all data]	0.1531
wR ₂ [all data]	0.2624
GOF	1.018
CCDC number	2092008

Supplementary Table 1 | Crystal Data and Structure Refinement for tris(helicene) B.

Supplementary Equation 1

$$W_{chiral} = \binom{N_{mol}}{N_{min}} = \frac{N_{mol}!}{(N_{mol}-N_{min})! N_{min}!} = \frac{N_{mol}!}{N_{maj}! N_{min}!}$$

Supplementary Equation 1 | Probability of including 'wrong' handedness Supplementary Eq. 1 gives the total number of possible arrangements for an ensemble in a solid solution of chiral molecules. It is assumed that the distribution of the molecules of opposite handedness (minorities) is random within every arrangement (independent of the surrounding node types and triangle sizes). N_{min} , N_{maj} and N_{mol} represent the numbers of minority molecules, majority molecules and total number of molecules ($N_{mol} = N_{maj} + N_{min}$), respectively.